


Article

GT Transcription Factors of *Rosa rugosa* Thunb. Involved in Salt Stress Response

Jianwen Wang [†] , Yufei Cheng [†], Xinwei Shi and Liguofeng ^{*}

College of Horticulture and Landscape Architecture, Yangzhou University, Yangzhou 225009, China

^{*} Correspondence: lgfeng@yzu.edu.cn; Tel.: +86-514-8797-1026

[†] These authors contributed equally to this work.

Simple Summary: Salt stress produced ion toxicity on plant cells and limited the of culture of cultivated *Rosa rugosa*. GT genes in salt stresses responses have been emerging. From the GT gene family of the salt-tolerant wild *Rosa rugosa*, four NaCl stress responsive genes (*RrGT-1*, *RrSIP1*, *RrSIP2*, *RrGTγ-4*) were identified. *RrSIP1* and *RrGTγ-4*, *RrGT-1* and *RrSIP2* located on chloroplasts and cell nucleus, respectively. *RrSIP1*, *RrSIP2* and *RrGTγ-4* could play roles in regulation of sodium and potassium transport. And *RrGT-1* expressed higher specifically in wild *Rosa rugosa* than in the salt-sensitive cultivated *Rosa rugosa*. These four genes would be candidates for further study of regulation mechanism of salt-tolerance of wild *Rosa rugosa* and would supply gene resources for tolerance improvement of cultivated *Rosa rugosa*.

Abstract: *Rosa rugosa* was a famous aromatic plant while poor salt tolerance of commercial cultivars has hindered its culture in saline-alkali soil. In many plants, the roles of GT (or trihelix) genes in salt stresses responses have been emerging. In the wild *R. rugosa*, a total of 37 GTs (*RrGTs*) were grouped into GT-1, GT-2, GTγ, SH4, and SIP1 lineages. SIP1 lineage expanded by transposition. The motifs involved in the binding of GT cis-elements were conserved. Four *RrGTs* (*RrGT11/14/16/18*) significantly differentially expressed in roots or leaves under salt stress. The responsive patterns within 8 h NaCl treatment indicated that *RrGTγ-4* (*RrGT18*) and *RrGT-1* (*RrGT16*) were significantly induced by salt in roots of *R. rugosa*. Subcellular localizations of *RrSIP1* (*RrGT11*) and *RrGTγ-4* were on chloroplasts while *RrGT-1* and *RrSIP2* (*RrGT14*) located on cell nucleus. Regulation of ion transport could be the most important role of *RrSIPs* and *RrGTγ-4*. And *RrGT-1* could be a halophytic gene with higher transcription abundance than glycophytic *GT-1*. These results provide key clue for further investigations of roles of *RrGTs* in salt stress response and would be helpful in the understanding the salt tolerance regulation mechanism of *R. rugosa*.

Keywords: *Rosa rugosa* Thunb.; GT or trihelix; halophytes



Citation: Wang, J.; Cheng, Y.; Shi, X.; Feng, L. GT Transcription Factors of *Rosa rugosa* Thunb. Involved in Salt Stress Response. *Biology* **2023**, *12*, 176. <https://doi.org/10.3390/biology12020176>

Academic Editors: Chengliang Sun and Weiwei Zhou

Received: 6 December 2022

Revised: 16 January 2023

Accepted: 19 January 2023

Published: 22 January 2023



Copyright: © 2023 by the authors. Licensee MDPI, Basel, Switzerland. This article is an open access article distributed under the terms and conditions of the Creative Commons Attribution (CC BY) license (<https://creativecommons.org/licenses/by/4.0/>).

1. Introduction

GT (or trihelix) family is a plant-specific transcription factor (TF) family with a DNA-binding domain rich in proline and glutamine residues [1,2]. The conserved DNA-binding domain containing three tandem helix structures (helix-loop-helix-loop-helix), namely trihelix domain [1,2]. The highly similar structure of trihelix domains and Myb/SANT-LIKE DNA-binding domains indicated that GT factors evolved from Myb/SANT-LIKE proteins [3]. GT elements are photosensitive cis-elements with A/T-rich motifs like '(T/A)-A-(T/A)' [4]. Interactions between GT factors and GT elements are implicated in the light dependent expression of many plant genes. e.g., the first identified GT gene *GT-1* binds two light-responsive elements of *Rubisco small subunit 3A* (*rbcS-3A*) of *Pisum sativum* L. [5]. A total of 30 GTs in *Arabidopsis thaliana* (L.) Heynh (*AtGTs*) were identified and classified into GT-1, GT-2, GTγ, SH4, and SIP1 lineages [6]. Most *AtGTs* played complex transcriptional

regulation roles in light-responsive gene regulation [7], immunity (*ARABIDOPSIS SH4-RELATED3*, *ASR3*) [8], perianth architecture regulation and fertility (*PETAL LOSS*, *PTL*) [9] and seed maturation (*Arabidopsis 6b-interacting protein 1-like 1*, *ASIL1*) [6]. Recently, roles of abiotic stress responses were identified in *GT* family, like *AtGTs* involved in salt-induced gene expression (*Arabidopsis GT-1-like transcription factor*, *GT-3A*) [10], hypoxia-responsive response (*AT3G10040*) [11] and salt and/or other abiotic stress tolerances (*Arabidopsis SIP1 clade Trihelix1*, *AST1*; *GT-4*, *GT2L*) [12–14]. Salt stress produced osmotic stress and ion toxicity on plant cells, resulting in the destruction of organelles and excess accumulation of activated oxygen [15,16]. Further, the photosynthesis decreasing and poor growth under salt stress contributed to the losses of quality and yield of economic crops [17]. The expression profile studies predicted some *GTs* which responded to salt stress in many crops, like cotton [18], wheat [19], *Brassica napus* L. [20], quinoa [21], *Sorghum bicolor* L. [22], soybean [23] and rice [24]. Function studies have proved salt tolerance regulation roles of several crop *GTs*. e.g., *OsGTγ-1* (*Os02g33770*) and *OsGTγ-2* (*Os11g06410*) of rice positively regulate salt tolerance [24]. *GmGT-2A*, *GmGT-2B* of soybean [25] and *GhGT26* of cotton [26] enhance salinity tolerance in overexpressed *Arabidopsis*.

Salinity stress is one of the most severe abiotic stresses and poses a continuing threat to economic crops [27], and for this reason the research are starting to consider and valorize wild species suitable for saline environments [28,29]. *Rosa rugosa* cultivars are widely used for spicery of food industry or essential oil of cosmetics industry [30,31]. These *R. rugosa* cultivars lost salt tolerance along with the breeding processes of floral traits, resulting in their limiting planting areas although there were vast saline-alkali soils in China [32–34]. e.g., the commercial cultivar *R. rugosa* ‘Zizhi’ (Zizhi) which planted in the narrow hilly lands of Shandong Province (China) was a typical glycophyte. While the wild *R. rugosa* which distributed naturally in the coastal area of northeast China belong to halophytes. The wild *R. rugosa* kept strong salt tolerance to adapt to the high salinity beach, as observed in other plant species in the coastal areas in the world [35]. In genetic engineering of salt-tolerance for glycophytic crop, homologous genes from halophytes should be more efficient since halophytes are more salt-tolerant than glycophytes [28,36]. The mining of salt responsive TF of wild *R. rugosa* would supply a base for salt tolerance improvement of *R. rugosa* cultivars [34].

With the genome of wild *R. rugosa*, this study aimed to screen *GTs* of *R. rugosa* (*RrGTs*) involved in the salt response. The phylogeny, synteny and sequence analyses would give a systematic understanding of lineage, gene duplication events, conserved motifs and gene structures of *RrGT* family. Expression profiles of salt treated *R. rugosa* were built to detect significantly induced/reduced *RrGTs*. These candidates were pointcuts of further study of salt stress responses regulation. Our study preliminary studied the roles of *RrGTs* under salt stress and would be helpful in understanding the regulatory mechanism of salt tolerance of *R. rugosa*.

2. Materials and Methods

2.1. Identification of *RrGT* Family

The *R. rugosa* and *Rosa chinensis* Jacq. genomes were obtained from GDR (Genome Database for Rosaceae, <https://www.rosaceae.org/>, accessed on 1 May 2022). Based on the hidden Markov model Myb/SANT-like DNA-binding domain (PF13837, <http://Pfam.sanger.ac.uk/>, accessed on 1 May 2022), candidate proteins were screened from the genome using HMMER 3.3.2 [37] with a cutoff threshold value of E-5. The ambiguous or incomplete candidates were rejected by TF verification of PlantTFDB (<http://planttfdb.cbi.pku.edu.cn/>, accessed on 1 May 2022).

2.2. Phylogenetic Analyses of *RrGT* Proteins

GT genes of *Oryza sativa* (*OsGTs*) and *Arabidopsis thaliana* were obtained from PlantTFDB (<http://planttfdb.cbi.pku.edu.cn/>, accessed on 1 May 2022). Based on the alignment of *GT* domains using MAFFT 7.55 (<https://mafft.cbrc.jp/alignment/server/>, accessed on

1 May 2022), a neighbor-join (NJ) phylogenetic tree was constructed by MEGA 7 with 1000 bootstrapping replications [38]. Besides, the p-distance model of the substitution type, pairwise deletion of Gaps/Missing data and uniform rates among sites were selected for the phylogenetic analysis.

2.3. Synteny Analysis of *RrGTs*

The homologous gene pairs ($E < 10^{-5}$, top five matches) within the *R. rugosa* genome or among *R. rugosa*, *R. chinensis* and *Fragaria vesca* L. genomes (obtained from GDR) were identified by BLASTP (BLAST+ 2.13.0) search. Based on the location of homologous pairs, MCScanX (mcscan2) [39] identified the syntenic regions and predicted the gene duplication events. *RrGTs* and corresponding homologous *GTs* on syntenic regions were highlighted by Synteny plot tool of TBtools [40].

2.4. Gene Structure, Motif Analysis and Cis-Acting Elements of *RrGT* Family

The top 10 conserved motifs were predicted by MEME web tools (<https://meme-suite.org/meme/>, accessed on 2 May 2022) under default parameters. Cis-elements on the 2000 bp sequence upstream to the initiation codon were predicted by PLANTCARE (<http://bioinformatics.psb.ugent.be/webtools/plantcare/html/>, accessed on 2 May 2022). The gene structures and motifs were illustrated by the Gene structure view tool of TBtools [40].

2.5. Expression Analysis under Salt Stress

Previous transcriptome data [32,41] of wild *R. rugosa* and *R. rugosa* ‘Zizhi’ provided the per kilobase of exon model per million mapped fragments (FPKM) of *RrGTs* and the fold-changes of differentially expressed *RrGTs*.

One-month-old wild *R. rugosa* seedlings were treated with 340 mM NaCl solution for 0.5 h, 1 h, 2 h, 4 h and 8 h and roots of these samples were collected with three biological repetitions. Total RNAs were extracted and reverse-transcribed as cDNA templates by RNAPrep Pure plant kit (Tiagen, Beijing, China) and HiScript[®] III RT SuperMix (Vazyme, Nanjing, China). Quantitative real-time polymerase chain reaction (qRT-PCR) was conducted using ChamQ SYBR Color qPCR Master Mix (Vazyme, Nanjing, China) on the CFX96 platform (Bio-Rad, China). All the steps of RNA extraction, reverse-transcription and qRT-PCR were conducted following the manufacturers’ recommended instructions. Table S5 listed the primers of *RrGTs* and reference genes (phD and 5.8s).

2.6. Subcellular Localization Analysis

The subcellular localization of *RrGTs* were predicted by webtools Plant-mPLOC (<http://www.csbio.sjtu.edu.cn/bioinf/plant-multi/>, accessed on 2 May 2022) and WoLF PSORT (<https://wolfpsort.hgc.jp/>, accessed on 2 May 2022). Coding sequences of 4 candidate *RrGTs* were cloned into 35S: green fluorescent protein (GFP) vector pNC-AMP-GFP-C and transformed to Arabidopsis protoplasts for overexpression of *RrGT*-GFP fusion proteins. The fluorescence of chloroplasts, GFP and 4′,6-diamidino-2-phenylindole (DAPI, Nuclear marker) were observed by the laser confocal microscopy.

3. Results

3.1. Lineages and Synteny of *RrGT* Family

A total of 37 *RrGTs* scattered across the seven chromosomes of *R. rugosa* genome (Figure 1B, Table S2). The NJ-tree of *RrGTs*, *OsGTs* and *AtGTs* divided 18, 7, 5, 4, 3 *RrGTs* to SIP1, GT-2, GT-1, SH4 and GT γ lineages, respectively (Figure 1A). The gene number of *RrGT* of each lineage is similar to that of *OsGTs* or *AtGTs* of corresponding lineage except SIP1 (Table S1).

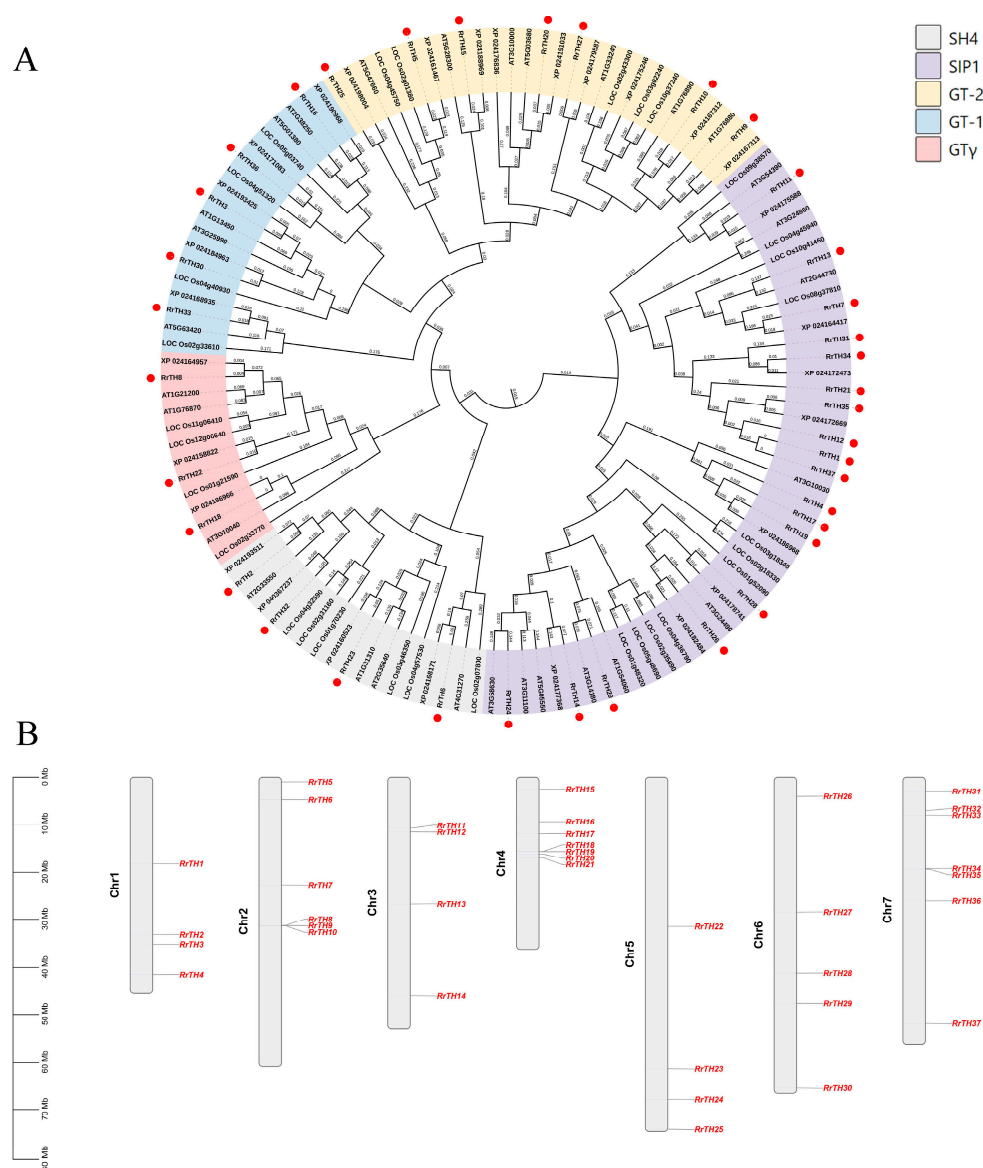


Figure 1. The phylogeny (A) and chromosome location (B) of GT family of *Rosa rugosa* (*RrGT*). The dendrogram of GTs of *R. rugosa*, *Rosa chinensis* (XP), *Oryza sativa* (LOC) and *Arabidopsis thaliana* (AT) was generated using the neighbor-joining method with 1000 bootstrap replicates (numbers in branches). Nodes were colored according to the five lineages of GT family and *RrGT*s were highlighted by red dots. The gene ID was listed in Table S2.

WGD (whole genome duplication) or segmental duplication produced three paralogous *RrGT* pairs, namely *RrTH2*-*RrTH32*, *RrTH3*-*RrTH30*, *RrTH26*-*RrTH28* on intra-species synteny regions of Chr1-Chr7, Chr1-Chr6 and Chr6-Chr6, respectively (Figure 2A, Tables S2 and S3) and 22 orthologous gene pairs of *RrGT*s-*RcGT*s (GTs of *R. chinensis*)-*FvGT*s (GTs of *F. vesca*) on inter-species synteny regions among *R. rugosa*, *R. chinensis* and *F. vesca* (Figure 2B, Table S2). Other *RrGT*s were predicted as ‘dispersed type’ which might arise from transposition and no tandem duplication events were identified. *RrTH12*, *RrTH30*, *RrTH32* produced five redundant homologous pairs on the synteny regions of non-homologous chromosomes (Figure 2B, red and green lines). After removing the small synteny regions which including less than 20 gene pairs (Figure S1), only one redundant pair was credible (Figure 2B, red line). The consistent collinearity indicated that the lineage evolution of GT families among *R. rugosa*, *R. chinensis* and *F. vesca* was conserved (Figure 2B).

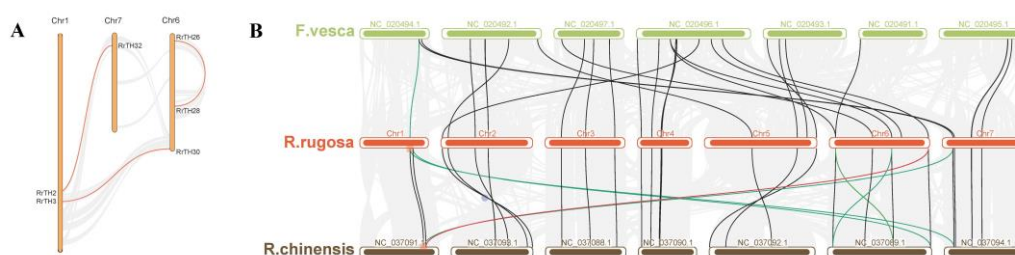


Figure 2. The intra-species (A) and inter-species (B) synteny of *RrGT* family. (A) The paralogous *RrGT*s on syntenic regions (dark lines) of chromosome 1/6/7. Three *RrGT* pairs are highlighted (Table S2). (B) Syntenic regions (dark lines) of genomes of *R. rugosa* (red), *Fragaria vesca* (green), *R. chinensis* (brown) and orthologous *GT*s (color lines). The orthologous *GT* pairs are linked by black lines. Green lines indicate *GT* pairs on overlapped syntenic regions.

It was worth noting that 7 *RrTH*s (*RrTH*1/4/12/17/21/31/37) of SIP1 lineage and *RrTH*10 of GT-2 lineage lacked homologous *GT*s in syntenic regions (Table S2). All these *RrTH*s in SIP1 lineage were dispersed type and it indicated transposition should contributed to the SIP1 lineage expansion of *R. rugosa*.

3.2. Gene Structures and Conserved Motifs of *RrGT* Family

The length of *RrGT* proteins varied from 199 to 896 amino acids (aa), with a molecular weight range of 21.977 (*RrTH*37) to 99.117 kDa (*RrTH*33). *RrGT* proteins of GT-2 lineage were longer due to their two trihelix domains. And the N-terminal trihelix domain (corresponding to the '7-5-10' motif group) was spaced from the C-terminal trihelix domain by motif 8. In other lineages, '2-5-1-4' motif group or '7-5-1-4' motif group constituted the trihelix domains (Figure 3, Table S4). Besides, motif 6, motif 9, motif 3 and motif 8 were specific to SIP1 lineage and GT-1/GT-2 lineage, respectively.

Over half *RrGT*s (20 *RrGT*s, 54.05%) included 2 exons and 10 *RrGT*s (27.03%) were intron-free. One *RrGT* contained 3, 7, 8 and 9 exons and two *RrGT* genes contained 5 exons, respectively. Exons of *RrGT*33 were up to 17 but most (exon 1–exon 12) coded the long nonconservative N-terminal with no conserved motifs.

3.3. Expression Analysis of *RrGT*s

In the RNA-seq expression profiles of wild *R. rugosa* under salt stress, 15 and 10 *RrGT*s were clustered as high- and middle-abundance genes, respectively (Figure 4, hierarchical clustering). In the 12 low abundant genes, except *RrGT*5/6/25/32 ($10 > \text{FPKM} > 1$) belonging to GT-2 and SH4 lineages, other 8 extremely low abundant *RrGT*s ($\text{FPKM} < 1$) were corresponding to the SIP1 lineage *RrGT*s without corresponding collinear *RcGT*s and *FvGT*s (Table S2).

Four differentially expressed genes were predicted as salt responsive *RrGT*s (Figure 4, red labeled *RrGT*s). Under salt stress, *RrTH*18 and *RrH*16 upregulated 16.19 fold in roots and 3.47 fold in leaves, respectively. *RrTH*11 and *RrTH*14 downregulated 0.35 fold, 0.36 fold in leaves, respectively (Table S2). The four candidate genes *RrTH*18, *RrTH*11, *RrTH*14 and *RrH*16 were named as *RrGT*γ-4, *RrSIP*1, *RrSIP*2 and *RrGT*-1, respectively.

The expression patterns of the four candidate genes were checked in wild *R. rugosa* seedlings treated by water (CK) and 340 mM NaCl solution (Figure 5). The salt responsive expression of *RrSIP*1 was down-regulated in 0.5 h, kept low abundance in 1 h and 2 h, then significantly up-regulated in 4 h and 8 h. Interestingly, water stress (CK) induced significant upregulation in 0.5 h and downregulation after 0.5 h of *RrSIP*1 which was opposite to its salt stress response. The expression of *RrSIP*2 only significantly downregulated in 2 h salt stress. The expression of *RrGT*-1 was stable before 2h then significantly upregulated to 19.08 fold in 8 h. *RrGT*γ-4 responded to salt stress tempestuously and rapidly. Its expression significantly upregulated to 14.5 fold from 1 h, reached 669 fold in 2 h then downregulated

to 8.2 fold in 8 h. Water stress also induced the upregulations of *RrGTγ-4* but the fold changes were far from induction of salt stress.

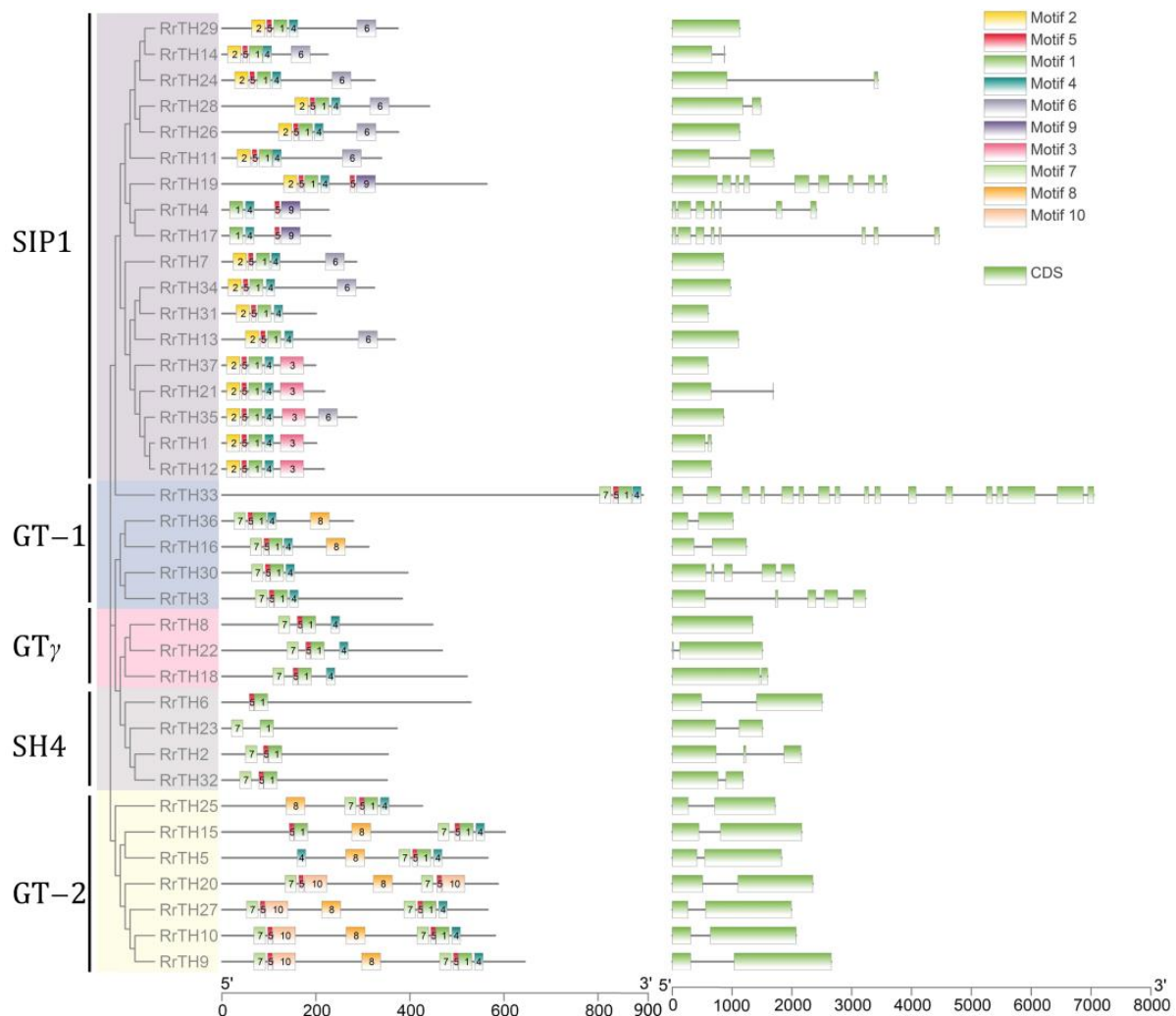


Figure 3. The conserved motifs and exon–intron structures of *RrGT* family. Five lineages are indicated by colored branches of NJ-dendrogram. The top 10 conserved motifs (boxes with numbers) were located by amino acid scale plate. The exons (green boxes) and introns (lines) were located by the nucleotide scale plate.

3.4. Subcellular Localization of *RrGT* Candidates

The predicted subcellular localizations (Table S2) of *RrGT* family were diverse (Nuclei, chloroplasts, mitochondria, cytoplasm and so on). And different prediction tools were inconsistent in prediction of several *RrGT*s. e.g., *RrSIP1* and *RrSIP2* were predicted as proteins located on nucleus by Plant-mPLOC but on chloroplasts by WoLF PSORT. We detected the subcellular localizations of above 4 candidates (*RrGTγ-4*, *RrSIP1*, *RrSIP2* and *RrGT-1*) to exclude the inconsistent prediction.

The fusion proteins of *RrSIP1*-GFP or *RrGTγ-4*-GFP (green) overlapped with chloroplasts (red) indicated that *RrSIP1* and *RrGTγ-4* were located on chloroplasts. The colocalizations (cyan) of fusion proteins (green) and nuclear marker (blue) indicated that *RrGT-1* and *RrSIP2* were located on nucleus (Figure 6).

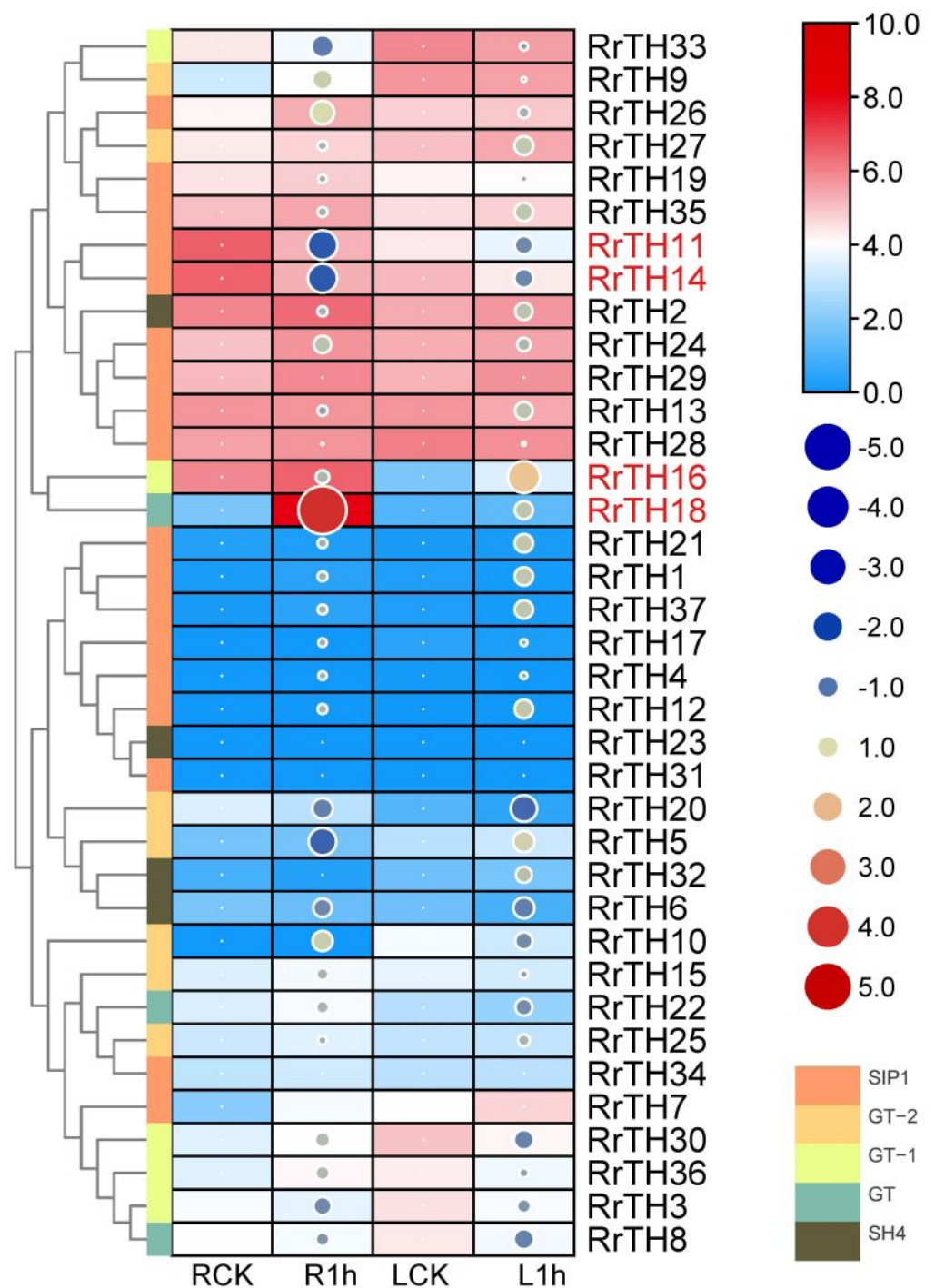


Figure 4. Expression profiles of *RrGTs* under salt stress in roots and leaves of *R. rugosa*. Four columns indicated roots or leaves of *R. rugosa* seedlings treated by NaCl solution (R1h or L1h) and water (RCK or LCK) for 1 h. Normalized FPKM (per kilobase of exon model per million mapped fragments) (Table S2) are indicated by the boxes with gradient colors. Log2(fold-change) (Table S2) using RCK and LCK as controls were indicated by size and gradient color of circles. Rows were clustered by hierarchical clustering of Euclidean distance. Five lineages were represented by colored nodes of clustergram. Differentially expressed *RrGTs* were labeled in red.

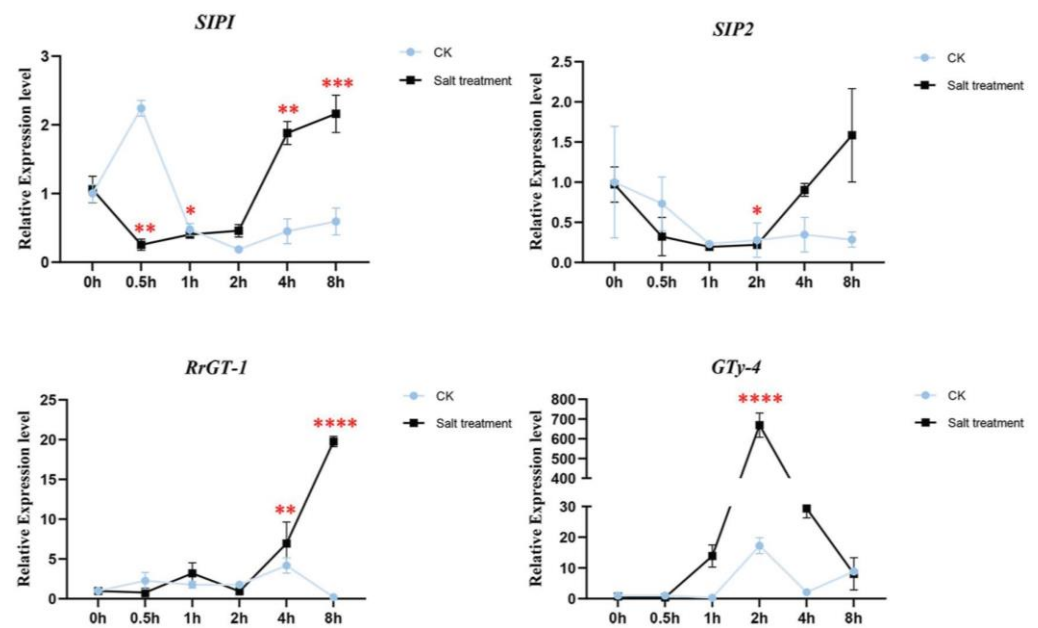


Figure 5. The salt responsive expression levels of *RrGTγ-4*, *RrSIP1*, *RrSIP2* and *RrGT-1* in roots of *R. rugosa*. The wild *R. rugosa* seedlings were treated by water (CK) and 340 mM NaCl solution (Salt treatment) from 0.5 h to 8 h. Untreated seedlings were the reference samples (0 h). *, **, *** and **** indicated the threshold value of significance of *t*-test 0.05, 0.01, 0.001 and 0.0001, respectively.

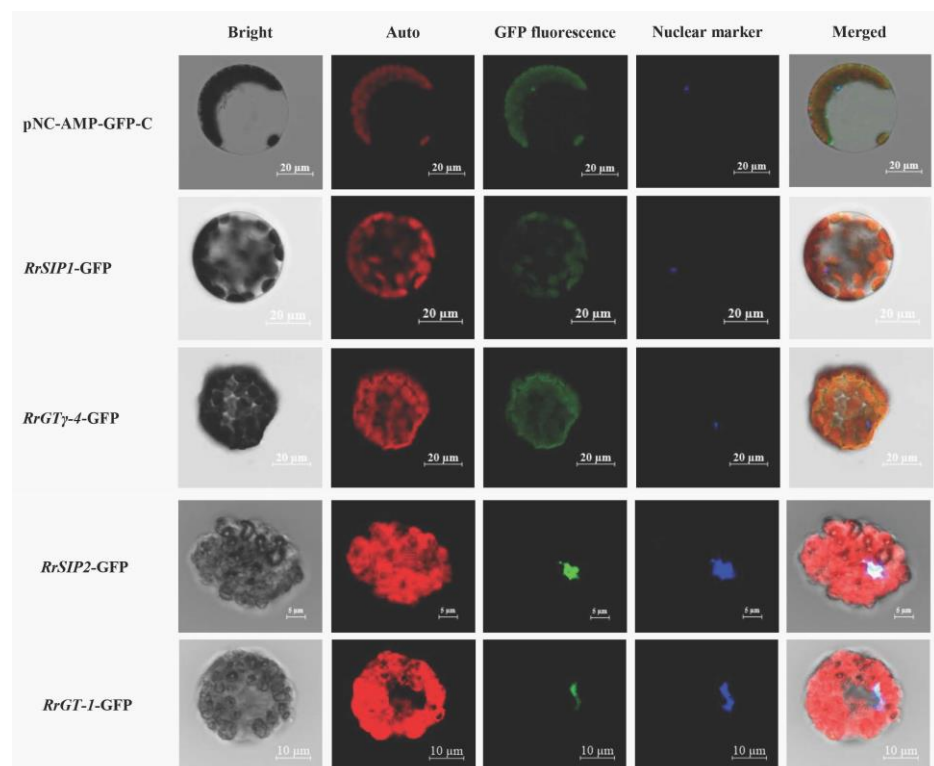


Figure 6. The subcellular localizations of *RrGTγ-4*, *RrSIP1*, *RrSIP2* and *RrGT-1*. Arabidopsis protoplasts transformed by GFP empty vector (pNC-AMP-GFP-C) or 35S: *GTs*-GFP vectors were observed using the laser confocal microscopy. The merged figures (Merged) were based on bright fields (Bright) and fluorescence of chloroplasts (Auto), green fluorescent protein (GFP), 4',6-diamidino-2-phenylindole (DAPI, Nuclear marker) on dark fields.

4. Discussion

4.1. The Species Specific Expansion of SIP1 Lineage

Expansion of SIP1 lineage has been observed in the *Brassica* plants. The majority of SIP1 genes of *Brassica rapa* L. retained two or three copies of corresponding *AtGTs* and it was more than other four lineages (one copy) [42]. The *Brassica* specific whole genome triplication contributed to the SIP1 lineage expansion since its divergence from *A. thaliana* [42,43]. But the conserved number of SIP1 genes of *R. rugosa* relative plants (8 *GTs* of *F. vesca* and 10 *GTs* of *R. chinensis*) indicated genome triplication or WGD did not contribute to *R. rugosa* SIP1 lineage expansion, and the specific expansion happened after the divergence from *R. chinensis* (Table S1). The 7 *RrGTs* (*RrTH1/12/17/21/31/37*) without corresponding collinear *RcGTs* and *FvGTs* were predicted as dispersed duplication types, which indicated proximal duplication and tandem duplication did not contribute to the SIP1 lineage expansion. And 5 of above genes (*RrTH1/12/21/31/37*) were clustered into the *Rosa*-specific lineages of the dendrogram with *RrTH34/35* and transcript abundances of the 5 genes were extremely low in roots and leaves (Figure 4). These observations indicated part of *RrGTs* in SIP1 lineage could arise from transposition, which contributed to SIP1 lineage expansion of *R. rugosa*.

4.2. Salt Responsive Candidates of *RrGTs*

In GT-1 lineage, *GT-3A* (*AT5G01380*) binds to GT elements of salt-induced *SCaM-4* gene (Ca²⁺-binding protein) of Arabidopsis and soybean [10]. The interaction of *GT-4* (*AT3G25990*) and *TEM2* (a B3 and AP2/ERF domain-containing protein) improved Arabidopsis salt tolerance by activating *Cor15A* (*AT2G42540*) [14]. *RrGT-1* clustered with *GT-3A* and *AT2G38250* (no reports on abiotic stress) in same cluster of GT-1 lineage (Figure 1). *RrGT-1* expressed much higher in roots (FPKM = 60.15) than in leaves (FPKM = 2.5). *RrGT-1* upregulated within 1 h salt stress only in leaves but strongly upregulated in roots under 8 h salt stress. The inconsistent inducing timing indicated *RrGT-1* responded to salt more promptly in leaves than in roots.

In *GTγ* lineage, *HRA1* (*HYPOXIA RESPONSE ATTENUATOR 1*, *AT3G10040*) attenuates the anaerobic response induced by ERF-VIIs by protein interaction with RAP2.12 [11]. In rice, three *OsGTγ* genes were induced by salt, abscisic acid (ABA) or other abiotic stresses [24,44]. *OsGTγ-1* was significantly induced by salt and its mutant increased salt stress sensitivity while *OsGTγ-1* overexpression enhanced salt tolerance [24]. Similar, knockout and overexpression of *OsGTγ-2* increased salt stress sensitivity and tolerance, respectively. In our study, *RrGTγ-4* clustered with *OsGTγ-1* and *HRA1* in same cluster of *GTγ* lineage. *RrGTγ-4* only highly expressed in roots under salt stress (FPKM = 271.54) and its abundance was much higher than other *RrGTs* (FPKM < 83). qRT-PCR proved the rapid and dramatic salt-inducing of *RrGTγ-4* in roots within 1 h and peaked at 2 h, which was similar to *OsGTγ-1*. *RrGTγ-4* should be a key candidate involved in salt tolerance regulation of *R. rugosa* roots.

In SIP1 lineage, *NtSIP1* was firstly identified from Agrobacterium 6b-interacting proteins of *Nicotiana tabacum* L. [45]. *AST1* (*At3g24860*) binds to a Novel AGAG-Box of stress tolerance genes to regulate Arabidopsis salt tolerance positively [12]. *BnSIP1-1* overexpression improved both osmotic and salt stresses tolerance during seed germination, but only improved osmotic stress tolerance of transgenic *B. napus* plants [20]. In our study, *RrSIP1*, *RrSIP2* were highly expressed in roots and leaves (FPKM > 20) and downregulated under salt stress only in leaves. Though most studies focus on stress induced GT genes, the two salt-stress-reduced *RrGTs* could be candidates involved in the negative regulation of salt tolerance.

Though no candidate *RrGTs* of GT-2 lineage significantly induced or reduced by salt, some studies have indicated GT-2 lineage also played roles in stress responses. e.g., Arabidopsis *gtl1* (*GTL1*, *AT1G33240*) mutant improved water use efficiency by reducing leaf transpiration [46], and *GT2L* (*AT5G28300*) induced significantly by salt, drought, cold and ABA and it responded to cold and salt stresses by interaction with calcium/calmodulin [13].

4.3. Potential Target Genes and Regulation Roles of *RrGTs*

Previous study indicated that *R. rugosa* responds to ion stress by gene expression regulation but rather gene dosage since its ion transporter gene number was conserved [34]. In rice, *OsGTγ-2* directly interacted with the GT-1 element 'GAAAAA' of three ion transporter genes (*OsHKT2*; 1, *OsNHX1* and *OsHKT1*; 3) [44]. In the ion transporter genes of the *R. rugosa*, GT-1 elements were found in the promoters (1000 bp upstream) of *RrHKT* (*evm.model.Chr5.2560*, only one *HKT* in the genome) and 6 of all 8 *RrNHXs* (*evm.model.Chr1.2289*, *evm.model.Chr1.4465* which is the only one *RrSOS1* [34], *evm.model.Chr2.1941*, *evm.model.Chr2.1942*, *evm.model.Chr4.416* and *evm.model.Chr5.7017*). Most transporter genes contained 1-4 GT-1 elements (-300 to -100 mostly) while only *evm.model.Chr5.7017* (*AtNHX5/6* homolog) identified 7 GT-1 elements all across the promoter (-700 to -100). It indicated that *RrGTγ-4* could be regulator of these ion transporter genes and coordinated ion transport under salt stress.

SIPs mostly take part in ABA signaling to resist growth inhibiting effect of salt stress. In apple, *MdSIP1-2* promoted lateral root development promotion which was associated with ABA sensitivity, drought and salt stress tolerance [47]. *AST1* and *BnSIP1-1* reduced water loss rate in the overexpressed seedlings [12,20]. The osmotic stress marker genes were highly expressed both in the *BnSIP1-1* transgenic plants and seedlings whereas ion transporter genes (*BnSOS1*, *BnNHX1*, and *BnHKT*) were only significantly higher expressed in transgenic seedlings (not in plants). *SIP* genes seem to exert different regulatory mechanisms along with different development process. Interestingly, the AGAG-Box 'GGTAAA' was found in two *RrNHXs* (*evm.model.Chr5.2640*, *evm.model.Chr4.534*) which lacked GT-1 elements. It indicated that excess ion response and plant developing regulation were crossed in *R. rugosa* by *RrSIPs*.

The genes of halophytes might be more superior for plant growth in saline-rich areas than their orthologs of glycophytes [28,29]. The 4 *RrGT* candidates were homologous to corresponding glycophytic *GTs* of Zizhi (over 90% protein identity). In roots, only *RrGT-1* (FPKM = 60.15, this study) expressed significantly higher than *GT-1* of Zizhi (FPKM = 2.34 [41]). *RrGT-1* could be a halophytic gene with higher transcription levels in wild *R. rugosa*. While the post translational regulation not transcription contributed mostly of salt-tolerance difference between halophytes and glycophytes. Whether the *GTs* were involved in the post translational regulation was not studied yet and it could be an important way to study the roles of other 3 *RrGTs* specific to halophytes [28,29].

5. Conclusions

In this study, we identified the *RrGT* family with 37 members from the *R. × rugosa* genome. *RrGTs* belonged to 5 lineages and *SIP1* lineage expanded significantly. The conserved motif groups corresponding to trihelix domains were most conserved. *RrGTγ-4* (*RrGT18*), *RrGT-1* (*RrGT16*) located on chloroplasts and *RrSIP1* (*RrGT11*), *RrSIP2* (*RrGT14*) located on nucleus. The four genes significantly differentially expressed under salt stress in roots or leaves. Regulation of ion transport could be the most important role of *RrSIP* genes and *RrGTγ-4* in response to salt stress of wild *R. rugosa*. And *RrGT-1* could be a halophytic gene with higher transcription abundance than glycophytic *GT-1*. Together, ion transport regulation roles of *GT* needed to be illuminated and the regulation role of *GTs* specific to halophytes would be a breakthrough point for further researches.

Supplementary Materials: The following supporting information can be downloaded at: <https://www.mdpi.com/article/10.3390/biology12020176/s1>. Figure S1: The synteny analysis of *RrGTs*, *RcGTs* and *FvGTs*; Table S1: Numer of *GT* genes of different plants; Table S2: Gene information, synteny analysis by MCscanX, RNA-seq and prediction of subcellular localizations of *RrGTs*; Table S3: The intra-species synteny regions; Table S4: Top 10 conserved motifs of *RrGT* family; Table S5: Primers for qRT-PCR.

Author Contributions: Conceptualization, J.W. and L.F.; Data curation, Y.C. and X.S.; Writing—Original draft, J.W.; Writing—Review & editing, J.W. and L.F. All authors have read and agreed to the published version of the manuscript.

Funding: The study was funded by the National Natural Science Foundation of China (grant numbers 32002076, 31972454, 32171861), the National Key R&D Program of China (grant number 2018YFD1000400), the Jiangsu Provincial Natural Science Foundation (grant number SBK2020043530), the Jiangsu Provincial Natural Science Research Project of Universities (grant number 20KJB210004), and the Jiangsu Provincial Agricultural Science and Technology Independent Innovation Fund (grant numbers CX(20)3023, CX(20)3026).

Institutional Review Board Statement: Not applicable.

Informed Consent Statement: Not applicable.

Data Availability Statement: Not applicable.

Conflicts of Interest: The authors declare no conflict of interest. The funders had no role in the design of the study; in the collection, analyses, or interpretation of data; in the writing of the manuscript; or in the decision to publish the results.

References

- Villain, P.; Mache, R.; Zhou, D.X. The mechanism of GT element-mediated cell type-specific transcriptional control. *J. Biol. Chem.* **1996**, *271*, 32593. [[CrossRef](#)] [[PubMed](#)]
- Zhou, D.X. Regulatory mechanism of plant gene transcription by GT-elements and GT-factors. *Trends Plant Sci.* **1999**, *4*, 210–214. [[CrossRef](#)] [[PubMed](#)]
- Nagano, Y. Several features of the GT-factor trihelix domain resemble those of the Myb DNA-binding domain. *Plant Physiol.* **2000**, *124*, 491–494. [[CrossRef](#)] [[PubMed](#)]
- Green, P.J.; Kay, S.A.; Chua, N.H. Sequence-specific interactions of a pea nuclear factor with light-responsive elements upstream of the *rbcS-3A* gene. *EMBO J.* **1987**, *6*, 2543–2549. [[CrossRef](#)]
- Green, P.J.; Yong, M.H.; Cuzzo, M.; Kano-Murakami, Y.; Silverstein, P.; Chua, N.H. Binding site requirements for pea nuclear protein factor GT-1 correlate with sequences required for light-dependent transcriptional activation of the *rbcS-3A* gene. *EMBO J.* **1988**, *7*, 4035–4044. [[CrossRef](#)] [[PubMed](#)]
- Gao, M.J.; Lydiate, D.J.; Li, X.; Lui, H.; Gjetvaj, B.; Hegedus, D.D.; Rozwadowski, K. Repression of seed maturation genes by a trihelix transcriptional repressor in Arabidopsis seedlings. *Plant Cell* **2009**, *21*, 54–71. [[CrossRef](#)]
- Murata, J.; Takase, H.; Hiratsuka, K. Characterization of a Novel GT-box Binding Protein from Arabidopsis. *Plant Biotechnol.* **2002**, *19*, 103–112. [[CrossRef](#)]
- Li, B.; Jiang, S.; Yu, X.; Cheng, C.; Chen, S.; Cheng, Y.; Yuan, J.S.; Jiang, D.; He, P.; Shan, L. Phosphorylation of trihelix transcriptional repressor ASR3 by MAP KINASE4 negatively regulates Arabidopsis immunity. *Plant Cell* **2015**, *27*, 839–856. [[CrossRef](#)]
- Brewer, P.B.; Howles, P.A.; Dorian, K.; Griffith, M.E.; Ishida, T.; Kaplan-Levy, R.N.; Kilinc, A.; Smyth, D.R. PETAL LOSS, a trihelix transcription factor gene, regulates perianth architecture in the Arabidopsis flower. *Development* **2004**, *131*, 4035–4045. [[CrossRef](#)]
- Park, H.C.; Kim, M.L.; Kang, Y.H.; Jeon, J.M.; Yoo, J.H.; Kim, M.C.; Park, C.Y.; Jeong, J.C.; Moon, B.C.; Lee, J.H.; et al. Pathogen- and NaCl-induced expression of the SCaM-4 promoter is mediated in part by a GT-1 box that interacts with a GT-1-like transcription factor. *Plant Physiol.* **2004**, *135*, 2150–2161. [[CrossRef](#)] [[PubMed](#)]
- Giuntoli, B.; Lee, S.C.; Licausi, F.; Kosmacz, M.; Oosumi, T.; van Dongen, J.T.; Bailey-Serres, J.; Perata, P. A trihelix DNA binding protein counterbalances hypoxia-responsive transcriptional activation in Arabidopsis. *PLoS Biol.* **2014**, *12*, e1001950. [[CrossRef](#)] [[PubMed](#)]
- Xu, H.; Shi, X.; He, L.; Guo, Y.; Zang, D.; Li, H.; Zhang, W.; Wang, Y. Arabidopsis thaliana Trihelix Transcription Factor AST1 Mediates Salt and Osmotic Stress Tolerance by Binding to a Novel AGAG-Box and Some GT Motifs. *Plant Cell Physiol.* **2018**, *59*, 946–965. [[CrossRef](#)] [[PubMed](#)]
- Xi, J.; Qiu, Y.; Du, L.; Poovaiah, B.W. Plant-specific trihelix transcription factor AtGT2L interacts with calcium/calmodulin and responds to cold and salt stresses. *Plant Sci.* **2012**, *185–186*, 274–280. [[CrossRef](#)]
- Wang, X.H.; Li, Q.T.; Chen, H.W.; Zhang, W.K.; Ma, B.; Chen, S.Y.; Zhang, J.S. Trihelix transcription factor GT-4 mediates salt tolerance via interaction with TEM2 in Arabidopsis. *BMC Plant Biol.* **2014**, *14*, 339. [[CrossRef](#)] [[PubMed](#)]
- Deinlein, U.; Stephan, A.B.; Horie, T.; Luo, W.; Xu, G.; Schroeder, J.I. Plant salt-tolerance mechanisms. *Trends Plant Sci.* **2014**, *19*, 371–379. [[CrossRef](#)] [[PubMed](#)]
- Zhang, J.L.; Shi, H. Physiological and molecular mechanisms of plant salt tolerance. *Photosynth Res.* **2013**, *115*, 1–22. [[CrossRef](#)]
- Yamaguchi, T.; Blumwald, E. Developing salt-tolerant crop plants: Challenges and opportunities. *Trends Plant Sci.* **2005**, *10*, 615–620. [[CrossRef](#)]

18. Magwanga, R.O.; Kirungu, J.N.; Lu, P.; Yang, X.; Dong, Q.; Cai, X.; Xu, Y.; Wang, X.; Zhou, Z.; Hou, Y.; et al. Genome wide identification of the trihelix transcription factors and overexpression of Gh_A05G2067 (GT-2), a novel gene contributing to increased drought and salt stresses tolerance in cotton. *Physiol. Plant* **2019**, *167*, 447–464. [\[CrossRef\]](#)
19. Wang, C.; Wang, Y.; Pan, Q.; Chen, S.; Feng, C.; Hai, J.; Li, H. Comparison of Trihelix transcription factors between wheat and Brachypodium distachyon at genome-wide. *BMC Genom.* **2019**, *20*, 142. [\[CrossRef\]](#)
20. Luo, J.; Tang, S.; Mei, F.; Peng, X.; Li, J.; Li, X.; Yan, X.; Zeng, X.; Liu, F.; Wu, Y.; et al. BnSIP1-1, a Trihelix Family Gene, Mediates Abiotic Stress Tolerance and ABA Signaling in Brassica napus. *Front. Plant Sci.* **2017**, *8*, 44. [\[CrossRef\]](#)
21. Li, K.; Fan, Y.; Zhou, G.; Liu, X.; Chen, S.; Chang, X.; Wu, W.; Duan, L.; Yao, M.; Wang, R.; et al. Genome-wide identification, phylogenetic analysis, and expression profiles of trihelix transcription factor family genes in quinoa (Chenopodium quinoa Willd.) under abiotic stress conditions. *BMC Genom.* **2022**, *23*, 499. [\[CrossRef\]](#)
22. Li, K.; Duan, L.; Zhang, Y.; Shi, M.; Chen, S.; Yang, M.; Ding, Y.; Peng, Y.; Dong, Y.; Yang, H.; et al. Genome-wide identification and expression profile analysis of trihelix transcription factor family genes in response to abiotic stress in sorghum [Sorghum bicolor (L.) Moench]. *BMC Genom.* **2021**, *22*, 738. [\[CrossRef\]](#)
23. Osorio, M.B.; Bucker-Neto, L.; Castilhos, G.; Turchetto-Zolet, A.C.; Wiebke-Strohm, B.; Bodanese-Zanettini, M.H.; Margis-Pinheiro, M. Identification and in silico characterization of soybean trihelix-GT and bHLH transcription factors involved in stress responses. *Genet. Mol. Biol.* **2012**, *35*, 233–246. [\[CrossRef\]](#)
24. Fang, Y.; Xie, K.; Hou, X.; Hu, H.; Xiong, L. Systematic analysis of GT factor family of rice reveals a novel subfamily involved in stress responses. *Mol. Genet. Genom.* **2010**, *283*, 157–169. [\[CrossRef\]](#)
25. Xie, Z.M.; Zou, H.F.; Lei, G.; Wei, W.; Zhou, Q.Y.; Niu, C.F.; Liao, Y.; Tian, A.G.; Ma, B.; Zhang, W.K.; et al. Soybean Trihelix transcription factors GmGT-2A and GmGT-2B improve plant tolerance to abiotic stresses in transgenic Arabidopsis. *PLoS ONE* **2009**, *4*, e6898. [\[CrossRef\]](#)
26. Li, Y.; Hu, Z.; Dong, Y.; Xie, Z. Trihelix Transcriptional Factor GhGT26 of Cotton Enhances Salinity Tolerance in Arabidopsis. *Plants* **2022**, *11*, 2694. [\[CrossRef\]](#)
27. Zhu, J.K. Plant salt tolerance. *Trends Plant Sci.* **2001**, *6*, 66–71. [\[CrossRef\]](#)
28. Himabindu, Y.; Chakradhar, T.; Reddy, M.C.; Kanygin, A.; Redding, K.E.; Chandrasekhar, T. Salt-tolerant genes from halophytes are potential key players of salt tolerance in glycophytes. *Environ. Exp. Bot.* **2016**, *124*, 39–63. [\[CrossRef\]](#)
29. Mishra, A.; Tanna, B. Halophytes: Potential Resources for Salt Stress Tolerance Genes and Promoters. *Front. Plant Sci.* **2017**, *8*, 829. [\[CrossRef\]](#)
30. Li, C.; Luo, Y.; Zhang, W.; Cai, Q.; Wu, X.; Tan, Z.; Chen, R.; Chen, Z.; Wang, S.; Zhang, L. A comparative study on chemical compositions and biological activities of four essential oils: *Cymbopogon citratus* (DC.) Stapf, *Cinnamomum cassia* (L.) Presl, *Salvia japonica* Thunb. and *Rosa rugosa* Thunb. *J. Ethnopharmacol.* **2021**, *280*, 114472. [\[CrossRef\]](#)
31. Cui, W.H.; Du, X.Y.; Zhong, M.C.; Fang, W.; Suo, Z.Q.; Wang, D.; Dong, X.; Jiang, X.D.; Hu, J.Y. Complex and reticulate origin of edible roses (*Rosa*, Rosaceae) in China. *Hortic Res.* **2022**, *9*, uhab051. [\[CrossRef\]](#)
32. Wang, J.; Zhang, W.; Cheng, Y.; Feng, L. Genome-Wide Identification of LATERAL ORGAN BOUNDARIES DOMAIN (LBD) Transcription Factors and Screening of Salt Stress Candidates of *Rosa rugosa* Thunb. *Biology* **2021**, *10*, 992. [\[CrossRef\]](#)
33. Tian, X.; Wang, Z.; Zhang, Q.; Ci, H.; Wang, P.; Yu, L.; Jia, G. Genome-wide transcriptome analysis of the salt stress tolerance mechanism in *Rosa chinensis*. *PLoS ONE* **2018**, *13*, e0200938. [\[CrossRef\]](#)
34. Zang, F.; Ma, Y.; Tu, X.; Huang, P.; Wu, Q.; Li, Z.; Liu, T.; Lin, F.; Pei, S.; Zang, D.; et al. A high-quality chromosome-level genome of wild *Rosa rugosa*. *DNA Res.* **2021**, *28*, dsab017. [\[CrossRef\]](#)
35. Perrino, E.V.; Signorile, G.; Marvulli, M. A first checklist of the vascular flora of the Polignano a Mare coast (Apulia, southern Italy). *Nat. Croat.* **2013**, *22*, 295–318.
36. Shabala, S. Learning from halophytes: Physiological basis and strategies to improve abiotic stress tolerance in crops. *Ann. Bot.* **2013**, *112*, 1209–1221. [\[CrossRef\]](#)
37. Potter, S.C.; Luciani, A.; Eddy, S.R.; Park, Y.; Lopez, R.; Finn, R.D. HMMER web server: 2018 update. *Nucleic Acids Res.* **2018**, *46*, W200–W204. [\[CrossRef\]](#)
38. Kumar, S.; Stecher, G.; Tamura, K. MEGA7: Molecular Evolutionary Genetics Analysis Version 7.0 for Bigger Datasets. *Mol. Biol. Evol.* **2016**, *33*, 1870–1874. [\[CrossRef\]](#)
39. Wang, Y.; Tang, H.; Debarry, J.D.; Tan, X.; Li, J.; Wang, X.; Lee, T.H.; Jin, H.; Marler, B.; Guo, H.; et al. MCScanX: A toolkit for detection and evolutionary analysis of gene synteny and collinearity. *Nucleic Acids Res.* **2012**, *40*, e49. [\[CrossRef\]](#)
40. Chen, C.; Chen, H.; Zhang, Y.; Thomas, H.R.; Frank, M.H.; He, Y.; Xia, R. TBtools: An Integrative Toolkit Developed for Interactive Analyses of Big Biological Data. *Mol. Plant* **2020**, *13*, 1194–1202. [\[CrossRef\]](#)
41. Wang, J.; Wang, P.; Xu, M.; Chen, Y.; Feng, L. Systematic Identification and Analysis of OSC Gene Family of *Rosa rugosa* Thunb. *Int. J. Mol. Sci.* **2022**, *23*, 13884. [\[CrossRef\]](#) [\[PubMed\]](#)
42. Wang, W.; Wu, P.; Liu, T.; Ren, H.; Li, Y.; Hou, X. Genome-wide Analysis and Expression Divergence of the Trihelix family in Brassica Rapa: Insight into the Evolutionary Patterns in Plants. *Sci. Rep.* **2017**, *7*, 6463. [\[CrossRef\]](#)
43. Liu, S.; Liu, Y.; Yang, X.; Tong, C.; Edwards, D.; Parkin, I.A.P.; Zhao, M.; Ma, J.; Yu, J.; Huang, S.; et al. The Brassica oleracea genome reveals the asymmetrical evolution of polyploid genomes. *Nat. Commun.* **2014**, *5*, 3930. [\[CrossRef\]](#)
44. Liu, X.; Wu, D.; Shan, T.; Xu, S.; Qin, R.; Li, H.; Negm, M.; Wu, D.; Li, J. The trihelix transcription factor OsGTγ-2 is involved adaption to salt stress in rice. *Plant Mol. Biol.* **2020**, *103*, 545–560. [\[CrossRef\]](#) [\[PubMed\]](#)

45. Kitakura, S.; Terakura, S.; Yoshioka, Y.; Machida, C.; Machida, Y. Interaction between *Agrobacterium tumefaciens* oncoprotein 6b and a tobacco nucleolar protein that is homologous to TNP1 encoded by a transposable element of *Antirrhinum majus*. *J. Plant Res.* **2008**, *121*, 425–433. [[CrossRef](#)] [[PubMed](#)]
46. Yoo, C.Y.; Mano, N.; Finkler, A.; Weng, H.; Day, I.S.; Reddy, A.S.N.; Poovaiah, B.W.; Fromm, H.; Hasegawa, P.M.; Mickelbart, M.V. A Ca(2+)/CaM-regulated transcriptional switch modulates stomatal development in response to water deficit. *Sci. Rep.* **2019**, *9*, 12282. [[CrossRef](#)]
47. Liu, H.F.; Zhang, T.T.; Liu, Y.Q.; Kang, H.; Rui, L.; Wang, D.R.; You, C.X.; Xue, X.M.; Wang, X.F. Genome-wide analysis of the 6B-INTERACTING PROTEIN1 gene family with functional characterization of MdSIP1-2 in *Malus domestica*. *Plant Physiol. Biochem.* **2023**, *195*, 89–100. [[CrossRef](#)]

Disclaimer/Publisher's Note: The statements, opinions and data contained in all publications are solely those of the individual author(s) and contributor(s) and not of MDPI and/or the editor(s). MDPI and/or the editor(s) disclaim responsibility for any injury to people or property resulting from any ideas, methods, instructions or products referred to in the content.